Application of Thermal CAE Analysis to Electric Drive Module for xEV

Michinari Fukuoka [1)] Yuki Fujita [1)] Masahiro Takemoto [1)] Yoshiyuki Kimura [1)]

1) DENSO CORPORATION, Kariya, Aichi, Japan

E-mail: michinari.fukuoka.j3a@jp.denso.com

ABSTRACT: This paper presents a method to construct 1D thermal model seamlessly from 3D thermal model to study the thermal performance and the approximate dimensions in the system study stage for the drive motor of xEV. Then, the current setting conditions of power control unit (PCU) for the electro-thermal coupling analysis are arranged with a view to studying the system and thermal establishment on a model basis with the customer.

KEY WORDS: electric vehicle, V-shaped process, model-based development, vehicle system simulation, power control unit, motor

1. INTRODUCTION

In recent years, all kinds of Electric Vehicle (xEV) such as batteries (BEV), hybrids (HEV), plug-in hybrids (PHEV), range extenders (REEV), and fuel cells (FCEV) have attracted a great deal of attention and are rapidly spreading around the world to reduce vehicle emissions.

In the development of a wide variety of electric drive systems, the V-shaped process is generally utilized in vehicle development. By linking hardware and software together, the process needs to be developed faster. One effective way to achieve this is to use model-based development (MBD) to improve the efficiency and speed of the complex system development. [(1) (2)]

In the V-shaped process shown in Figure 1, DENSO is using MBD to verify the system on a computer from the initial design stage and to judge the performance of the vehicle across fields such as electric drive and cooling systems. Furthermore, by combining the core and customization settings shown in Figure 2 with design automation, the efficiency and quality of component design are improved. Through these efforts, we aim to not only reduce the design lead time by minimizing the repetition of prototyping and measurements, but also to make optimal proposals for the system as a comprehensive system supplier.

In this paper, for the drive motor, we first propose a method to construct 1D thermal model seamlessly from 3D thermal model to study the thermal performance and the approximate dimensions in the system study stage. Next, for the power control unit (PCU), the current setting conditions for the electro-thermal coupling analysis, which will be required as a common language, are arranged with a view to studying the system and thermal establishment on a model basis with the customer.

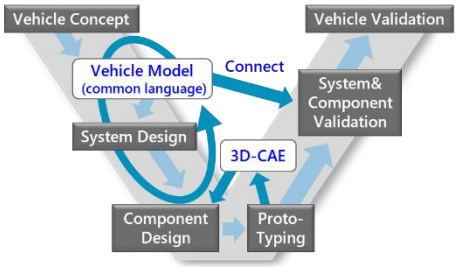

Fig. 1 MBD utilization in V-shaped process.

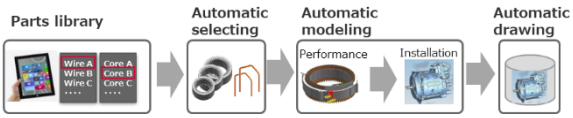

Fig. 2 Core and customization settings and design automation.

2. 1D Thermal Model Construction

2.1. 1D Thermal Model Construction Flow

In this chapter, we propose a method to construct a 1D thermal model seamlessly from a 3D thermal model.

Figure 3 shows the flow of 1D thermal model construction based on the calculation results of an arbitrary 3D thermal model. From the temperature difference ΔT and heat flux Q_{th} between the parts obtained by 3D thermal calculation, the thermal resistance R_{th} between the parts is given by

$$R_{th} = \Delta T \,/\, Q_{th}. \quad (1)$$

Using the obtained thermal resistance, a thermal resistance network is constructed based on the component arrangement. Then, the calculation results between the thermal resistance network and the 3D thermal model are compared to calibrate the resistance of the gap between the stator and the rotor, and the heat flux due to radiation Q_{thr} is implemented from

$$Q_{thr} = \sigma\epsilon\left(T_p^4 - T_a^4\right), \quad (2)$$

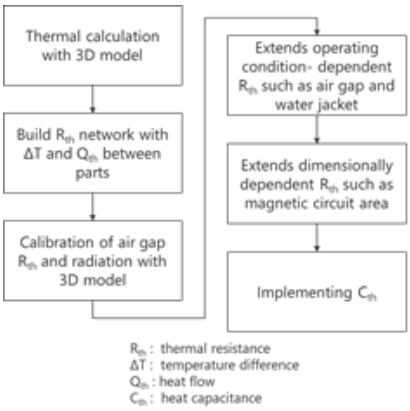

Fig. 3 1D thermal model construction flow.

where the Stefan-Boltzmann coefficient is σ, the emissivity is ϵ, the temperature of the arbitrary parts surface is T_p, and the facing temperature of the parts is T_a, respectively.

Then, the thermal resistance depending on the operating state, such as the rotor speed and the volume flow rate, is extended based on the theoretical formula. In general, the thermal resistance R_{th} determined by the convection is given by

$$R_{th} = 1 \,/\, hS, \tag{3}$$

where heat transfer coefficient h, and the heat transfer area is S, respectively. Here, the gap thermal resistance varies with the rotor speed and is given by

$$h = N_u \lambda \,/\, L\,, \tag{4}$$

where the Nusselt number is N_u, the thermal conductivity is λ, and the representative length is L, respectively. Since the gap exists uniformly in the circumferential direction at a fixed distance, it can be regarded as a parallel flat plate, and the Nusselt number is given by Equations 5 to 7 for laminar and turbulent flows.[3]

$$\text{At laminar flow;} \quad N_u = C_1 P_r^{1/3} R_e^{1/2}, \tag{5}$$

$$\text{At turbulent flow;} \quad N_u = C_2 P_r^{1/5} R_e^{4/5}, \tag{6}$$

$$R_e = vL \,/\, \nu, \tag{7}$$

where the constants are C_1 and C_2, the Prandtl number is P_r, the Reynolds number is R_e, the velocity is v, and the kinematic viscosity is ν, respectively. It is laminar when R_e is less than 32,000. Also, the gap flow v_g is geiven using the rotor speed N,

$$v_g = \pi D N, \tag{8}$$

where the gap diameter is D. From Equation 3 to 8, the thermal resistance R_{thg} of the gap is arranged by,

$$R_{thg} \propto 1 \,/\, N^{1/2} \text{ at laminar, } 1 \,/\, N^{4/5} \text{ at turbulent,} \tag{9}$$

Equation 9 shows that the gap thermal resistance is proportional to the 1/2 power of the rotor speed in the laminar, and to the 4/5 power of the speed in the turbulent. Equation 9 makes the gap thermal resistance a variable of the rotor speed.

Similarly, the velocity v_w of the cooling water is given using the volumetric flow rate Q_w as follows;

$$v_w = Q_w \,/\, S_w, \tag{10}$$

where the channel cross section is S_w. From Equations 3 to 7 and 10, the channel thermal resistance R_{thw} is arranged as follows;

$$R_{thg} \propto 1 \,/\, {Q_w}^{1/2} \text{ at laminar, } 1 \,/\, {Q_w}^{4/5} \text{ at turbulent,} \tag{11}$$

Equation 11 makes the channel thermal resistance a variable of the volumetric flow rate.

In addition, the thermal resistance of the part that varies with the product thickness and diameter of the magnetic circuit part is extended. Finally, heat capacity C_{th} is implemented in the thermal resistance network using below,

$$C_{th} = \rho c V, \tag{12}$$

where the density is ρ, the volumetric specific heat is c, and the volume is V.

The above flow made it possible to construct a 1D thermal model depending on operating conditions and dimensions using the temperature difference and heat flux between the parts extracted from the 3D thermal model.

2.2. Calculated results of Constructed 1D Thermal Model

Figure 4 shows the outline of the constructed 1D thermal model. The target motor is a PM motor with a cooling channel in the stator housing, and wires, stator cores and magnets are the main sources of heat generation. The lines connecting the parts indicate thermal resistance, and except for the air gap between the wire and the magnet, the air in the enclosure, which has a small effect on part temperature, was ignored. Here, since water-cooled motors generally have the highest temperature at the end winding, the accuracy of temperature prediction was improved by dividing the wire and the end winding.

Figure 5 shows the temperature comparison results between 3D and constructed 1D thermal model which include before and after calibration. In general, in 3D thermal models such as the finite element method or the finite volume method, fluid regions such as air are often calculated as one region. On the other hand, in the 1D thermal model, only the thermal resistance of the gap is modeled for higher accuracy, and since the subject of calculation of the air

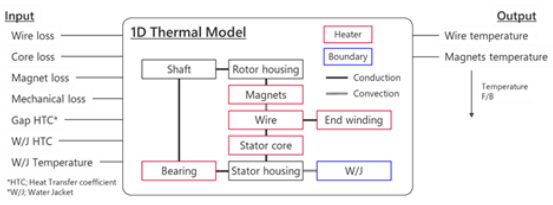

Fig. 4 Schematic of constructed 1D thermal model.

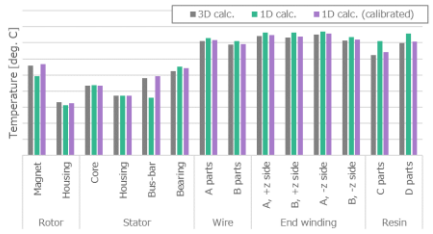

Fig. 5 Comparison of calculated temperatures.

region is different between the 3D and 1D thermal model, it is difficult to calculate the thermal resistance by Equation 1. In this study, the thermal resistance of the gap was calibrated to match the calculated results of the 3D thermal model using a parameter study. In addition, heat flux due to radiation was implemented for components whose temperature difference from the 3D thermal model deviated by more than 10 degrees Celsius from the 1D thermal model temperature calculation result after calibrating the gap resistance. By calibrating the gap thermal resistance and implementing heat flux of radiation, the 3D and 1D thermal model are agreement well with the temperature estimation results.

Figure 6 shows the transition of maximum temperatures of the magnet and wire during five runs in the WLTC mode as calculated by the constructed 1D thermal model. The figure shows how the wire temperature, which is the main heat source, fluctuates following the change in the loss according to the change in running speed. Also, because the magnet has a large heat capacity, the temperature gradually increases throughout the five mode runs.

3. Standardization of PCU Thermal Analysis Conditions

3.1. Overview

A power control unit (PCU) needs to ensure thermal performance for a wide variety of operating conditions and also satisfy the required heat resistance life. In order to verify these, it is necessary to accurately predict the temperature transition of the

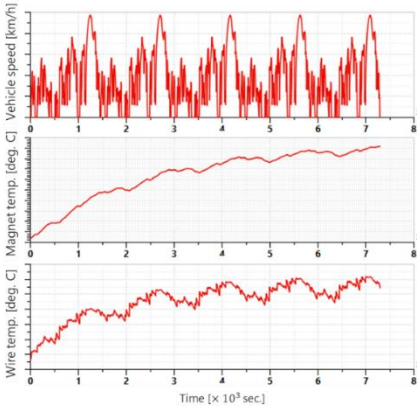

Fig. 6 Magnet temperature transition during WLTC.

heat-resistant parts relative to the actual running pattern, but it is not always easy to accurately predict the temperature of each parts because PCU have a large number of parts and heat generation sites are scattered.

Here, the smoothing capacitor element, the current sensor element, and each resin component are heat-resistant bottleneck parts in the PCU. And these are affected by the temperature of the connection terminal between the PCU and the motor or battery, and by the wind flow in the mounting position. Therefore, it is necessary to accurately understand these boundary conditions in order to accurately evaluate the heat resistance performance of each part.

On the other hand, these boundary conditions are determined by the thermal balance between the PCU and the components connected to the PCU, as well as the running condition of the vehicle. In the past, boundary conditions were determined by referring to similar systems in the past or measurement results from the previous development phase, but there were issues such as excessive thermal quality and design rework caused by exceeding the heat resistance temperature.

To address this issue, as exemplified by MILS (Model In the Loop Simulation), there is a method that utilizes vehicle system simulation using a thermal plant model of each component under design to calculate boundary conditions between components and reflect them in each component design.

Figure 7 shows a schematic of a vehicle system model that can simultaneously verify power and thermal performance. By utilizing this model, the battery SOC (Stage of charge), Motor Generator (MG)/PCU output, or the flow rate and temperature of the cooling circuit can be calculated to verify the required specifications of the system for any driving pattern.

On the other hand, in order to calculate the heat resistance performance and life of the internal parts, a thermal plant model that can perform high-speed calculations while covering the internal parts is required. In particular, PCU with a large number of parts tend to have a larger thermal model scale, so it is necessary to reduce the model scale by using 1D models or reduced order models (ROM), and systematization of thermal calculation methods is required.

In order to accurately predict the temperature distribution in each part of the PCU, it is necessary to conduct coupled electro-thermal analysis to consider the bus-bar heat generation distribution. This chapter clarifies how to give the effective value of the current at each site, which is necessary for the electro-thermal coupling analysis of PCU.

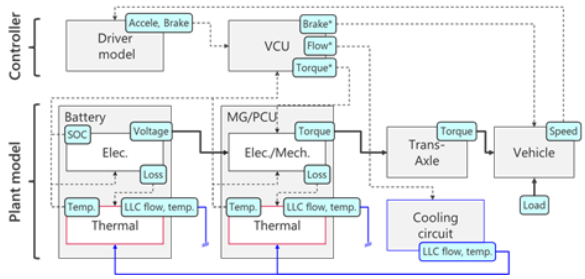

Fig. 7 Schematic of the vehicle system model.

3.2. PCU currents for the electro-thermal coupling analysis

Figure 8 shows inverter circuit including a step-down circuit as an example of a PCU circuit. For each variable in the figure, I_b is the battery current, I_L is the reactor current, I_L' is the current after boosting, I_{ch} is the ripple current of the smoothing capacitor, and I_m is the MG current, respectively. Here, in a circuit with a step-down switching element, it is common to combine the switching elements in one place in order to facilitate cooling, and the circuit in Figure 8 can be rewritten in Figure 9. The figure shows that the current must be insulated on the bus-bar in the electro-thermal coupling analysis because the continuous condition of the current is not established between the smoothing capacitor and the switching element.

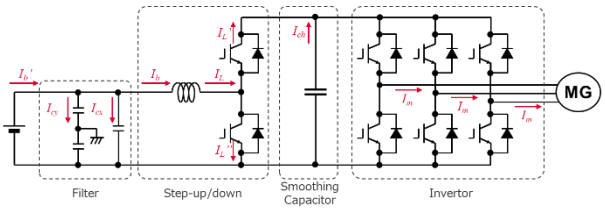

Fig. 8 PCU circuit including step-up/down convertor.

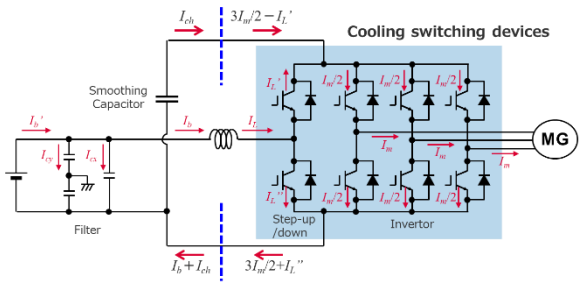

Fig. 9 PCU circuit rewritten from structure.

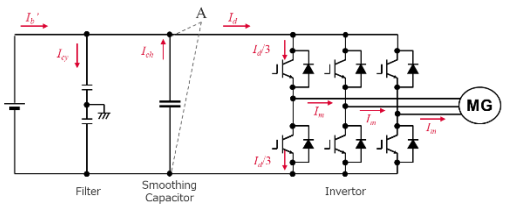

Fig. 10 Inverter circuit.

Figure 10 shows a typical inverter circuit as an example of a PCU circuit. I_d in the figure is the effective value of the sum of I_b and I_{ch}. Here, at point A in the figure, since the sum of I_b and I_{ch} does not agree with I_d in the effective value of current, there is A point where the continuity of current does not hold. Therefore, in the electro-thermal coupling analysis, it is found that the current needs to be insulated near the contact point between the smoothing capacitor and the bus-bar through which the main current flows.

4. Conclusion

In this paper, we propose a method to construct a 1D thermal model seamlessly from a 3D thermal CAE model as a method to examine the heat capacity of the drive motor and to examine the approximate dimensions at the system examination stage, aiming at improving the efficiency and shortening of the V-shaped process. Next, for the power control unit (PCU) used in various electric drive systems, the current setting conditions for the electro-thermal coupling analysis were arranged with a view to studying the system and thermal establishment on a model basis with the customer.

In the future, we will accelerate model-based development using methods for constructing 1D thermal models of motors and vehicle system simulations that utilize current conditions, leading to higher overall system quality and contributing to the reduction of vehicle emissions.

5. Acknowledgements

The authors would like to thank Tetsuya Akino and Hiroshi Ohi (TOYOTA MOTOR CORPORATION) for helpful discussions about standardization of the inverter thermal analysis.

REFERENCES

(1) K. Minami, “Development methodologies to deliver “Differentiation” under rapid shift to EV,” *Ansys Simulation World 2022*, A-6, Sep. 2022.

(2) P. Dini, S. Saponara, “Electro-Thermal Model-Based Design of Bidirectional On-Board Chargers in Hybrid and Full Electric Vehicles,” *Electronics 2022*, 11(1), 112, Dec. 2021.

(3) The Japan Society of Mechanical Engineers, “Heat Transfer Engineering Materials Revised 5th Edition,” pp. 27-29, May 2009. (In Japanese.)